

This article was downloaded by:

On: 25 January 2011

Access details: *Access Details: Free Access*

Publisher *Taylor & Francis*

Informa Ltd Registered in England and Wales Registered Number: 1072954 Registered office: Mortimer House, 37-41 Mortimer Street, London W1T 3JH, UK



## Separation Science and Technology

Publication details, including instructions for authors and subscription information:

<http://www.informaworld.com/smpp/title~content=t713708471>

### Determination of Solid Deformation Effect on the Effective Diffusivity During Extraction from Plants

Ilona Seikova<sup>a</sup>; Evgeni Simeonov<sup>a</sup>

<sup>a</sup> Department of Chemical Engineering, University of Chemical Technology and Metallurgy, Sofia, Bulgaria

Online publication date: 09 August 2003

**To cite this Article** Seikova, Ilona and Simeonov, Evgeni(2003) 'Determination of Solid Deformation Effect on the Effective Diffusivity During Extraction from Plants', *Separation Science and Technology*, 38: 15, 3713 – 3729

**To link to this Article:** DOI: 10.1081/SS-120024225

URL: <http://dx.doi.org/10.1081/SS-120024225>

## PLEASE SCROLL DOWN FOR ARTICLE

Full terms and conditions of use: <http://www.informaworld.com/terms-and-conditions-of-access.pdf>

This article may be used for research, teaching and private study purposes. Any substantial or systematic reproduction, re-distribution, re-selling, loan or sub-licensing, systematic supply or distribution in any form to anyone is expressly forbidden.

The publisher does not give any warranty express or implied or make any representation that the contents will be complete or accurate or up to date. The accuracy of any instructions, formulae and drug doses should be independently verified with primary sources. The publisher shall not be liable for any loss, actions, claims, proceedings, demand or costs or damages whatsoever or howsoever caused arising directly or indirectly in connection with or arising out of the use of this material.

## Determination of Solid Deformation Effect on the Effective Diffusivity During Extraction from Plants

Ilona Seikova\* and Evgeni Simeonov

Department of Chemical Engineering, University of Chemical  
Technology and Metallurgy, Sofia, Bulgaria

### ABSTRACT

A short-cut method was developed to account for the swelling effect on the effective diffusion coefficient during the course of a solid–liquid extraction. Exemplary, the kinetics of alkaloid recovery from the plant *Atropa belladonne* in batch stirred vessel was reported. Supporting experiments were performed to obtain the solid volume modification that is associated with the kinetics of solvent penetration. The volume of the solvent-impregnated solid was changed by a factor of 1.4 to 1.7 during extraction. The analytical solutions of the model for a diffusion controlled process were checked with the experimental kinetics to determine the effective diffusion coefficients. The values varied between  $3.68 \times 10^{-10} \text{ m}^2\text{s}^{-1}$  and  $4.79 \times 10^{-10} \text{ m}^2\text{s}^{-1}$  (when considering volume

---

\*Correspondence: Ilona Seikova, Department of Chemical Engineering, University of Chemical Technology and Metallurgy, 8 blvd. Kliment Ohridski, 1756 Sofia, Bulgaria; E-mail: saykovs@yahoo.com.

3713

DOI: 10.1081/SS-120024225  
Copyright © 2003 by Marcel Dekker, Inc.

0149-6395 (Print); 1520-5754 (Online)  
www.dekker.com

modification) and between  $2.52 \times 10^{-10} \text{ m}^2 \text{s}^{-1}$  and  $3.45 \times 10^{-10} \text{ m}^2 \text{s}^{-1}$ , under constant volume system hypothesis. To interpret the difference between the effective diffusivities, a correction term was derived accounting for the geometric factors variations. The swelling was found to be three dimensional and the correction term, giving the relative volume change to power values of 0.666, produced a good fit with the experimental data.

## INTRODUCTION

One of the most commonly used approaches for calculation of the effective diffusion coefficient during solid–liquid extraction is based on the determination of the experimental kinetics for a periodically led diffusion-controlled process. Concentration in liquids phase vs time data have been usually measured, and fitted to theoretical models under appropriate hypotheses, to yield values of the kinetic parameters. The general mass-transfer model is formulated through the conservation law of mass of solute within the heterogeneous porous medium, where the diffusion process is analyzed using the diffusion flux relative to the mass or volume average velocity.<sup>[1–3]</sup>

The mathematical model consists of differential mass transfer of the solute

$$\frac{\partial(\varepsilon_p C_p)}{\partial t} + V \cdot \nabla C_p - \varepsilon_p \cdot \nabla D \cdot \nabla C_p = 0 \quad (1)$$

coupled with the overall continuity equation:

$$\frac{\partial(\varepsilon_p \rho)}{\partial t} + \nabla \cdot (\rho V) = 0 \quad (2)$$

The convection term involving the velocity in the pores  $V$  in the diffusional direction is necessary in cases of a large change in density, porosity, and swelling of the material due to the solvent adsorption.

When the fluid is incompressible, Eq. (1) is given in dimensionless form as follows:

$$\frac{\partial(\varepsilon_p C_p)}{\partial \theta} + u \cdot \nabla C_p - \frac{1}{Pe_d} \varepsilon_p \cdot \nabla \bar{D} \cdot \nabla C_p = 0 \quad (3)$$

using as a dimensionless variable the time parameter  $\theta = tU/R_p$ ,  $u = V/U$ , where  $U$  is a characteristic velocity in the pores and  $Pe_d = R_p U / D_0$ , which is related to the ratio of diffusion time  $t_{dif} (= R_p^2 / D_0)$  to the characteristic time of penetration in pores of the particles  $t_p (= R_p / U)$ . Under assumption of  $Pe_d \ll 1$  (at low velocities and fast kinetics of extraction), the

convection term  $u \cdot \nabla C_p$  may be neglected, and the dispersion is governed by molecular diffusion. The dependence of the diffusive mass transfer on the porous structure is taken into account by the effective diffusion coefficient  $D_{eff}$ .

$$\varepsilon_p D = D_{eff} = \frac{\varepsilon_p D_M}{\tau} \quad (4)$$

The internal porosity  $\varepsilon_p$  and the tortuosity  $\tau$  are macroscopic properties of nonideal porous media describing respectively, the relative effective pore volume and the relative average length of the flow path in the diffusional direction.

Different approaches (parametric as well a nonparametric) to obtain the concentration and porosity dependent diffusivity were proposed to include the structural modifications with increasing the extraction.<sup>[4,5]</sup> In a previous study, the mathematical model of the process, accounting for the concentration dependent diffusivity and variable porosity, was stated and solved numerically.<sup>[6]</sup> The modeling results show that for low concentration ranges (dilute solution and low initial solute content) and predominant macro-porosity, the consideration of variable diffusivity is more significant only in the initial, steep part of the kinetic curve. For larger times, characterized by a very small increase in extraction rate for the extraction systems investigated, the effect of the variable diffusivity on the kinetic behavior may be neglected.

In the present work, we studied the swelling effect associated with solvent adsorption during direct extraction of alkaloidic salts from the plant *Atropa belladone*. To predict such extraction processes, we present here an approximation method for the calculation of kinetic curves and the estimation for the swelling effect on the effective diffusion coefficient. The method is based on the analytical solution of the diffusion-controlled removal in the Regular regime, when the diffusion coefficient is constant and the rate of extraction is slowly influenced by the initial conditions. The effect of volume modification was studied by comparing diffusion coefficients when considering or neglecting volume increase. The objective of the comparative analysis was to derive a corrective term for geometry variation in the effective diffusion coefficient.

## KINETICS MODELING

Extraction is presumed to occur under the following conditions.

1. The dispersed solid material is an assembly of spherical particles of the same size.



2. The solution is highly diluted and there are no dissolution limits; the saturation concentration is high compared to the actual concentration of the solvent in the pore.
3. Solvent penetration in the pores during swelling occurred at low velocity.
4. The porous structure is characterized by a predominant macro-porosity and the dependence on pore radius is neglected.
5. The solute in the particle is transported by diffusion. This is described by a constant diffusion coefficient inside a variable volume system.

When the amount of extractable solute is quantified of terms of its mass fraction  $X_s$ , Eq. (1) becomes:

$$\frac{\partial(X_s \rho_{ap})}{\partial t} = \nabla(D_{eff} \nabla X_s \rho_{ap}) \quad (5)$$

where  $\rho_{ap}$  is the apparent density of particle (mass/volume of solid + pores filled with solvent). For a constant volume system the equation takes the form:

$$\frac{\partial X_s}{\partial t} = \nabla(D_{eff} \nabla X_s) \quad (6)$$

For finite batch conditions, the basic diffusion model is completed by the overall mass balance assuming perfect mixing in the extractor vessel:

$$\beta(X_{s,o} - \bar{X}_s) = Y - Y_0 \quad (7)$$

where  $Y$  is a solute mass fraction in the continuous phase and  $\beta$  represents the ratio of the volume of solvent in pores of particles  $V_{ls}$  to that in the bulk liquid phase  $V_l$ . The volume-averaged solid phase fraction is calculated from:

$$\bar{X}_s(t) = \frac{3}{R_{p,0}^3} \int_0^{R_{p,0}} X_s(r, t) r^2 dr \quad (8)$$

Mathematical solution of Eq. (6) gives the fraction of extracted amount at time  $t$  to the maximum amount of extractable compounds at the initial state.<sup>[7,8]</sup>

$$E(t) = \frac{X_{s,0} - \bar{X}_s}{X_{s,0}} = \frac{1}{1 + \beta} - \sum_{n=1}^{\infty} B_n \exp\left(-\frac{\mu_n^2 D_{eff} t}{R_{p,0}^2}\right) \quad (9)$$



Under conditions of strong diffusion control, the parameters of the analytical solutions are defined as:<sup>[7]</sup>

$$B_n = \frac{6}{\mu_n^2 + 9\beta(1 + \beta)} \quad (10)$$

where  $\mu_n$  are the positive roots of the characteristic equation

$$\tan \mu_n = \frac{3\mu_n\beta}{3\beta + \mu_n^2} \quad (11)$$

and show the strong effect of the phase ratio  $\beta$ .

When considering the change in volume of a solid, substituting  $\rho_{ap} = ms/V_{sl}$ , we have

$$\frac{\partial \left( m_s \frac{X_s}{V_{sl}} \right)}{\partial t} = \nabla \left( D_{eff} \nabla \left( m_s \frac{X_s}{V_{sl}} \right) \right) \quad (12)$$

where  $m_s$  and  $V_{sl}$  denote the mass of the solid and the apparent volume occupied by the particle (solid + pores filled with solvent) accessible through solvent penetration measurement. Supposing that the amount extracted is negligible in respect to the total mass ( $ms \approx \text{const}$ ), Eq. (12) is expressed as:

$$\frac{\partial X_{ap}}{\partial t} = \nabla (\tilde{D}_{eff} \nabla X_{ap}) \quad (13)$$

with the apparent concentration  $X_{ap} = X_s/V_{sl}$ . The solution of this equation is given by:

$$E(t) = \frac{X_{ap,0} - \bar{X}_{ap}}{X_{ap,0}} = \frac{1}{1 + \tilde{\beta}} - \sum_{n=1}^{\infty} \frac{6}{\mu_n^2 + 9\tilde{\beta}(1 + \tilde{\beta})} \times \exp \left( -\frac{\mu_n^2 \tilde{D}_{eff} t}{R_p^2} \right) \quad (14)$$

where  $R_p$  is a particle radius in any time  $t$ . From Eqs. (9) and (14), the theoretical relation between  $E(t)$  and the characteristic time for internal diffusion  $t_{dif}$  is derived, which can be compared with the experimental data to obtain the values of effective diffusion coefficients when considering or neglecting volume increase.



## EXPERIMENTAL

Vegetable alkaloid recovery from the medicinal plant *Atropa belladonna* is reported as an example. Tropan alkaloids are in alkaloidic salt form and are extracted directly by dissolution in polar solvent.<sup>[19]</sup> The initial content of alkaloids obtained after continuous extraction in a Soxhlet apparatus reaches up to 0.6 to 0.1% from the dried mass. The experiments performed with a single particle indicate that during extraction, the geometry of the sample shifts from irregular to regular sphere shape accompanied by sensible increase in linear dimension. The change is attributed to the significant content of starch, which can reach 15%. During extraction, solvent was adsorbed by the swelling of the starch granules and this process continues during the whole stage of extraction.

The structure of the porous solid was investigated by nitrogen adsorption at 77.4°K by the simplified single-point BET procedure. The results show that the pore space is characterized by a predominant macroporosity with mean pore radius of 16 nm and low internal free superficies (specific area  $0.4 \text{ m}^2 \text{ g}^{-1}$ , free volume  $0.15 \text{ cm}^3 \text{ g}^{-1}$ ).

The experimental procedure was divided in two groups. The first one analyzed the recovery of the alkaloids in the cleaned – up extracts to provide the experimental kinetics. The alkaloid concentration was recorded by spectrophotometric measurement at wavelength  $\lambda = 430 \text{ nm}$ .<sup>[10,11]</sup> The second group investigated the kinetics of solvent penetration. For this aim, during determined intervals of time, the extraction was stopped and after filtration the mass of solvent-impregnated solid ( $m_{sl}$ ) was weighed on a digital balance to an accuracy of  $\pm 0.001 \text{ g}$ . The solvent was eliminated from the solid in the drying unit at 40°C for about 12 hours to constant weight  $m_{ss}$ . Because the mass of solute and cosolute extracted are negligible in respect to the initial mass of solid  $m_s$ , the changes in the mass of the dried solid  $m_{ss}$  may be neglected. The volume of solvent penetrated into the porous material  $V_{ls} = f(t)$  can be determined by noting that:

$$V_{ls}(t) = \frac{m_{sl}(t) - m_s}{\rho_1} \quad (15)$$

The extraction kinetics was studied under periodical conditions in a thermostated stirred vessel under the following conditions: extracting agent, 10% water solution of ethanol; liquid–solid ratio  $\xi = 0.01 \text{ m}^3 \text{ kg}^{-1}$ ; and angular velocity  $n = 5 \text{ s}^{-1}$ ; which eliminates the external mass-transfer resistance. Kinetics experiments were performed at temperatures of 25°C



and 40°C using fractions with mean size of  $2 \times 10^{-3}$  m and  $4 \times 10^{-3}$  m from the milled roots of the plant.

## RESULTS AND DISCUSSION

### Kinetics of Solvent Penetration

The volume modifications as a function of time for the two particle sizes at a temperature of  $T = 25^\circ\text{C}$  and at  $T = 40^\circ\text{C}$  are reported in Figure 1 and Figure 2, respectively. The deformation is reported in terms of the relative change  $v_V$  considering that the rise in solid volume equalizes the solvent volume filled the pores of particles  $V_{ls}$ :

$$v_V = \frac{\Delta V}{V_{s,0}} = \frac{V_{ls}}{V_{s,0}} \quad (16)$$

The exponential fit, presented in Figure 1 and Figure 2, is derived from the equation

$$v_V(t) = v_{V,\infty}(1 - \exp^{-H_V t}) \quad (17)$$

where the value of  $v_{V,\infty}$  at the end of a run and the exponential adjustable constant  $H_V$  varied with the operating conditions (Table 1). There is

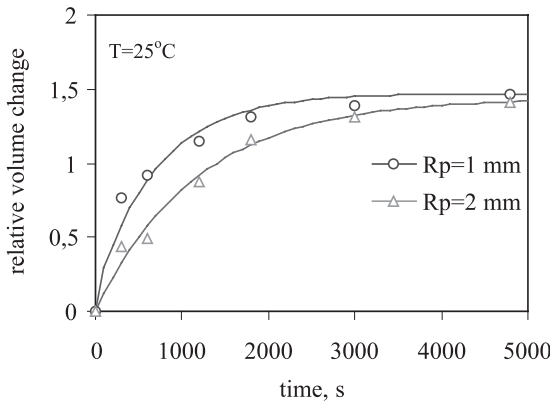


Figure 1. Effect of particle size on relative volume change  $v_V$ .



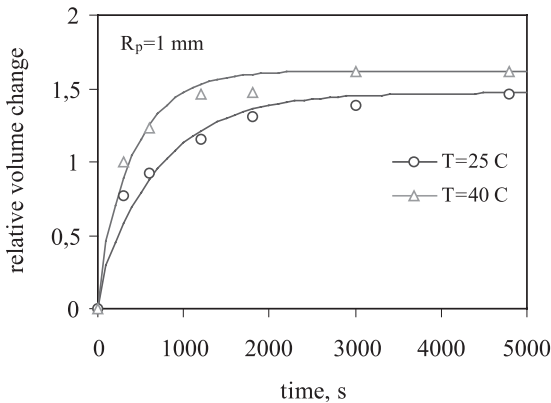


Figure 2. Effect of temperature on relative volume change  $v_V$ .

clearly a substantial increase in the apparent volume of solid at all experimental conditions. The course of the dependants and the identified values of the fitting parameter  $H_V$  indicate that the kinetics of penetration is faster for the fraction with a smaller size or at higher temperature.

To verify the assumption of  $Pe_D \ll 1$  for the purely diffusive mass transfer Eq. (3) from the experimental kinetics of solvent penetration, the radial velocity in the pores was estimated. The overall continuity equation, Eq. (2), considering only the radial flow direction, gives:

$$\frac{\partial(\rho \varepsilon_p)}{\partial t} + \frac{1}{r^2} \frac{\partial}{\partial r} (r^2 \rho U_r) = 0 \quad (18)$$

After integration with respect to the radial position from  $r=0$  to  $R_p$ , the volume-averaged radial velocity in the pores  $U_r$  can be obtained.<sup>[2]</sup>

$$U_r = \frac{R_p}{3\rho} \frac{d(\rho \varepsilon_p)}{dt} \quad (19)$$

Inserting the function  $\varepsilon_p = f(t)$  and noting  $\varepsilon_p = v_V/(1 + v_V)$ , we can derive an empirical relationship for the penetration velocity:

$$U_r = \frac{R_p}{3} \frac{H_V v_{V,\infty} \exp^{-H_V t}}{(1 + v_V)^2} \quad (20)$$

**Table 1.** Model parameters used in the calculation.

	T = 25°C; $R_p = 1$ mm	T = 25°C; $R_p = 2$ mm	T = 40°C; $R_p = 1$ mm
$H_V, \times 10^3 \text{ s}^{-1}$	1.385	0.837	3.423
$v_{V,\infty}$	1.47	1.44	1.62
$D_{eff}, \times 10^{10} \text{ m}^2\text{s}^{-1}$	2.94	2.52	3.45
$\tilde{D}_{eff}, \times 10^{10} \text{ m}^2\text{s}^{-1}$	4.26	3.68	4.79
$\tilde{D}_{eff}, \times 10^{10} \text{ m}^2\text{s}^{-1}$	4.05	3.46	4.87

In Figure 3, we plot the variation of  $U_r$  vs time for each of the three sets of data in Figures 1 and 2. The calculations demonstrated that only for very small times of rapid variation in the porosity, the penetration velocity accedes the ranges of  $10^{-7} \text{ ms}^{-1}$ . The results suggest that the condition  $Pe_D \gg 1$  is especially validated for the larger times in the case of moderate particle size ( $10^{-3} \text{ m}$ ) and moderately fast diffusion ( $10^{-10} \text{ m}^2\text{s}^{-1}$ ).

#### Calculation of Effective Diffusion Coefficients

Having obtained the time evolution of the volume  $V_{sl} = f(t)$  and of the extracted alkaloid amount  $m_{ext} = f(t)$  from the overall mass balance Eq. (7), under the condition of initially solute-free solvent), the normalized solute

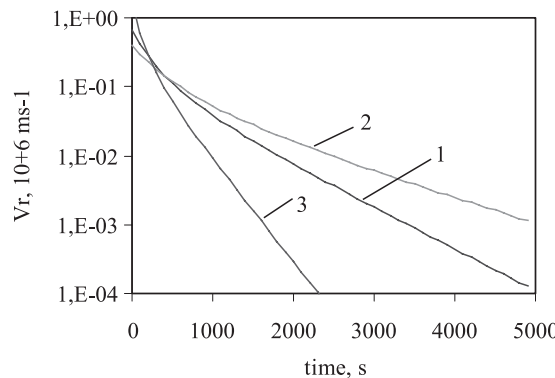


**Figure 3.** Volume averaged velocity of solvent penetration vs time (1:  $T = 25^\circ\text{C}$ ;  $R_p = 1 \times 10^{-3} \text{ m}$ ; 2:  $T = 25^\circ\text{C}$ ;  $R_p = 2 \times 10^{-3} \text{ m}$ ; 3:  $T = 40^\circ\text{C}$ ;  $R_p = 1 \times 10^{-3} \text{ m}$ ).



mass fractions extracted and not extracted were calculated when neglecting the volume variation, as

$$X^* = \frac{\bar{X}_s}{X_{s,0}} = \frac{(m_{so} - m_{ext})/m_s}{m_{so}/m_s} \quad Y^* = \frac{Y}{X_{s,0}} = \frac{m_{ext}/m_s}{m_{so}/m_s} \quad (21)$$

when volume variation is considered:

$$X_{ap}^* = \frac{\bar{X}_{ap}}{X_{ap,0}} = \frac{(m_{so} - m_{ext})/V_{sl}}{m_{so}/V_{s,0}} \quad Y_{ap}^* = \frac{Y_{ap}}{X_{ap,0}} = \frac{m_{ext}/V_1}{m_{so}/V_{s,0}} \quad (22)$$

The analytical solutions of the model were checked with the experimental kinetics to determine the effective diffusion coefficients. As an example, the experimental and calculated data from Eqs. (14) and (22) (considering volume variation) are presented in Figure 4 for the experiment with a particle size  $R_p = 1 \times 10^{-3}$  m at a temperature of 25°C. For comparison, the calculated data from Eqs. (9) and (21) (ignoring volume variation) are reported in Figure 5. The different shape of the kinetic curves is evident when considering or neglecting the volume evolution: in respect to  $X^*$ , the decrease in  $X_{ap}^*$  in the solid phase is corrected by the ratio  $V_{s,0}/V_{sl}$ , which decreases with the time, and respectively, in the liquid phase, in respect to  $Y$ , the increase  $Y_{ap}^*$  is proportional to the increasing ratio  $V_{s,0}/V_1$  when the swelling effect is taken into account.

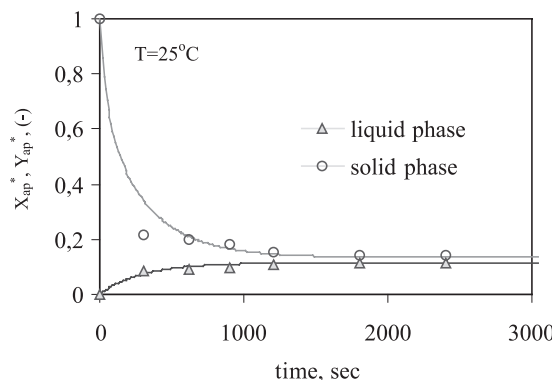


**Figure 4.** Experimental and calculated dimensionless concentration as a function of time, considering volume modifications ( $T = 25^\circ\text{C}$ ;  $R_p = 1 \times 10^{-3}$  m;  $\zeta = 0.01 \text{ m}^3 \text{ kg}^{-1}$ ).

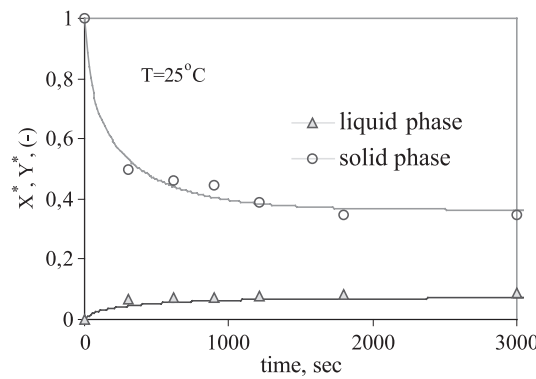


**Figure 5.** Experimental and calculated reduced fractions as a function of time, neglecting volume modifications ( $T = 25^\circ\text{C}$ ;  $R_p = 1 \times 10^{-3}$  m;  $\xi = 0.01 \text{ m}^3 \text{ kg}^{-1}$ ).

The lines shown in the Figure 4 and Figure 5 represents the best fits to the experimental data. As seen in the figures, very good fits were achieved for all cases presented, but each pair of kinetic curves for the same experimental conditions were characterized by a different value of the diffusion coefficient. The identified values of the adjustable parameters,  $D_{\text{eff}}$  and  $\tilde{D}_{\text{eff}}$ , are reported in Table 1. Analyzing the predicted values of the coefficients, similar behavior in relation to the operation parameters was observed, considering or neglecting the swelling effect. The increase in effective diffusivity was observed when the temperature was increased from  $25^\circ\text{C}$  to  $40^\circ\text{C}$ , as well as when smaller-sized particles were used. The values obtained for  $D_{\text{eff}}$  from a constant volume system were lower than the diffusion coefficients  $\tilde{D}_{\text{eff}}$ , when considering the swelling effect, which was expected. To obtain the same rate of extraction at a larger particle size an increased effective diffusivity has to be used in the model.

#### Estimation for Swelling Effect on the Diffusion Coefficients

Using the Regular regime concept, when only the first term of the infinite-series solution is considered, an approximate value for  $\tilde{D}_{\text{eff}}$  can be derived that accounts for the increase in particle size. It is known that the experimental kinetic data can be described accurately by a three-parametric exponential function resulting from the analytical solution:<sup>[12,13]</sup>

$$E(t) = E_\infty - B \exp^{-Ht} \quad (23)$$



where  $B$  and  $H$  are empirically adjustable constants, and  $E_\infty$  is a maximum extract fraction reached at equilibrium. The time derivative from the experimental kinetic curve, Eq. (23), and from the analytical solution, Eq. (9) is given by:

$$\left(\frac{dE}{dt}\right)_{\text{exp}} = -H(E_\infty - E(t)) \quad (24)$$

$$\frac{dE}{dt} \approx -\frac{\mu_1^2 \bar{D}_{\text{eff}}}{\bar{R}_p^2} (E_\infty - E(t)) \quad (25)$$

where  $\bar{D}_{\text{eff}}$  is an approximate value for the effective diffusivity for a constant averaged volume  $V_{s,av}$  that corresponds on the mean particle size  $\bar{R}_p$ :

$$\bar{R}_p = R_{p,0} + 0.5(R_{p,\infty} - R_{p,0}) \quad (26)$$

Swelling during extraction was assumed to be almost three dimensional and the mean particle size was calculated from the relative volume increase:

$$\frac{\bar{R}_p}{R_{p,0}} = 0.5(1 + (1 + v_{V,\infty})^{1/3}) \quad (27)$$

In region of Regular regime, where Eq. (25) is valid, the effective diffusion coefficient can be estimated from:

$$\bar{D}_{\text{eff}} = \frac{HR_p^2}{\mu_1^2} \quad (28)$$

where for infinite batch conditions and no external resistance, the limit value of  $\mu_1 = \pi$  can be used. This expression has the same form as that obtained by the standard function technique for a constant volume system.<sup>[12]</sup> Taking as a reference the yielded diffusivity for constant volume system, the values for the effective diffusion coefficients corrected for the size effect is estimated from:

$$\bar{D}_{\text{eff}} = D_{\text{eff}}[0.5(1 + (1 + v_{V,\infty})^{1/3})]^2 \quad (29)$$

The effect of the correction factor can be illustrated by the slopes of the relationship between the kinetic rate  $dE/dt$  and the driving force  $E_\infty - E(t)$ . From the exact solutions Eqs. (9) and (14) for the yielded kinetic parameters values (Table 1), the relation  $dE/dt - (E_\infty - E)$  was obtained, and compared, as shown in Figure 6.

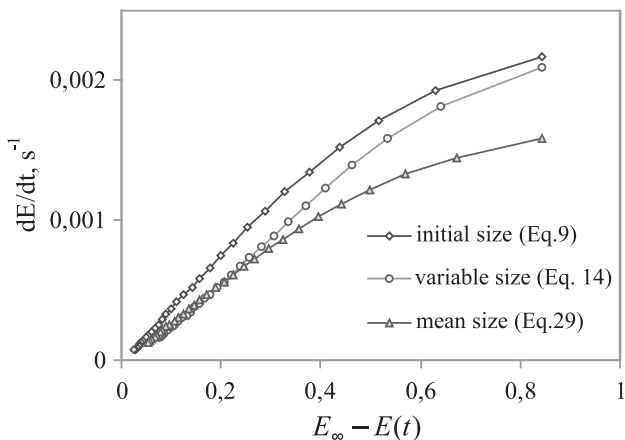


**Figure 6.** Kinetics rate vs driving force for different model hypotheses ( $T = 25^\circ\text{C}$ ;  $R_{p,0} = 1 \times 10^{-3} \text{ m}$ ;  $\xi = 0.01 \text{ m}^3 \text{ kg}^{-1}$ ).

Two kinetic periods were distinguished: the initial part of the extraction process, where the curves diverge significantly, and the second stage, where an essentially linear relationship can be seen for both cases of invariable particle size. The change in the trend of the curves occurs around the starting point of Regular regime, given by the condition  $tD_{\text{eff}}/R_p^2 > 0.1$  for the limiting case of a purely diffusional infinite batch process.<sup>[7]</sup> For the fast kinetics examined, this condition is ascertained for very small times of  $t \approx 300 \text{ s}$  and  $E \approx 0.6$ . This figure also shows that in regions of Regular regime, the curve calculated using Eqs. (27) through (29) merge with the curve deduced from Eq. (14) under variable  $R_p$  and  $\beta$ . The driving forces for mass transfer were similar and diminished more slowly in respect to those of the initial particle size.

The sensibility of the kinetic curves toward the model hypotheses is illustrated in Figure 7. The comparison of experimental and calculated data is reported for the run at  $40^\circ\text{C}$ , but the results presented can be regarded as representative of all operating conditions. A tailing-to-the-end characterizes the kinetic curve when a parallel effect of volume increase is taken into account (curve 2). The effect resulted from the increase in the diffusion path with the advancement of the extraction. The approximation of constant particle volume with initial particle size (curve 1) gives a faster kinetics of extraction with lower equilibrium value. The prediction with a diffusion coefficient corrected for the size effect, Eq. (29), approaches with acceptable accuracy the experimental data (curve 3). The second part of



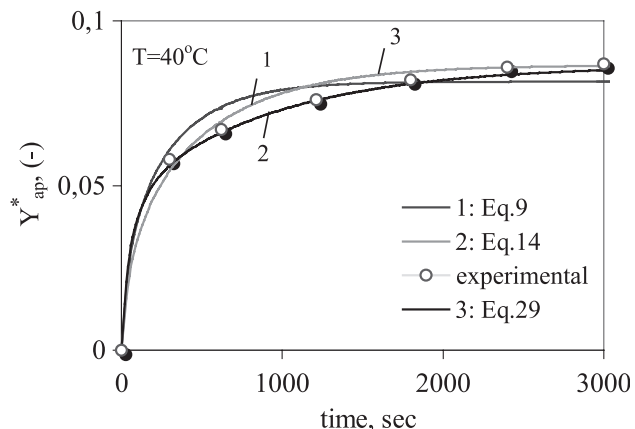


**Figure 7.** Calculated kinetic curves for different model hypotheses 1:  $D_{eff}$  ( $V_{s,0} = const$ ); 2:  $\bar{D}_{eff}$  [ $V_{sl} = f(\eta_V)$ ]; 3:  $\bar{D}_{eff}$  ( $V_{sl} = V_{av}$ ). ( $T = 40^\circ\text{C}$ ;  $R_{p,0} = 1 \times 10^{-3}$  m;  $\xi = 0.01 \text{ m}^3 \text{ kg}^{-1}$ ).

the curve is predicted with greater error because the diffusional path increase in the approximate formula Eqs. (26) and (27) was half of the actual particle size variation at the end of the process.

## CONCLUSION

The observation concerning the extraction from the plant *Atropa belladonna* demonstrated an increase in the effective diffusivity when a parallel effect of swelling is observed. This effect can be reported in the concentration term, substituting the initial solid volume by the apparent volume of the solid (solid + pores filled with solvent). Accounting for the increasing volume and particle size, a tailing-to-the-end of the kinetic curve may be predicted with more confidence.

An approximate method to estimate the volume modification effect was proposed where the effective diffusivity for constant volume system is corrected to include geometry variation. The correction term accounting for the relative volume change at power values of 0.666 gives an acceptance estimation of the effect of increase in volume during extraction. The approach presented may be expected to fit data for kinetics of extraction only when the concentration dependency on the diffusion coefficient is negligible.

## NOMENCLATURE

$B$	empirical constant in Eq. (23) $\text{kg kg}^{-1}$
$C_p$	concentration in pores of particle, $\text{kg m}^{-3}$
$D$	intraparticle dispersion coefficient, $\text{m}^2 \text{s}^{-1}$
$\bar{D}$	dimensionless dispersion coefficient in Eq. (3)
$D_{eff}$	effective diffusivity (considering constant volume), $\text{m}^2 \text{s}^{-1}$
$\tilde{D}_{eff}$	effective diffusivity (considering variable volume), $\text{m}^2 \text{s}^{-1}$
$\bar{D}_{eff}$	effective diffusivity (considering averaged volume), $\text{m}^2 \text{s}^{-1}$
$D_M$	molecular diffusivity, $\text{m}^2 \text{s}^{-1}$
$E$	fraction of extracted compound defined in Eq. (9), $\text{kg kg}^{-1}$
$H$	empirical constant in Eq. (23), $\text{s}^{-1}$
$H_v$	fitting parameter in Eq. (17), $\text{s}^{-1}$
$m_{ext}$	mass of solute in the extract, kg
$m_s$	initial mass of solid, kg
$m_{so}$	initial mass of extractable compound, kg
$m_{sl}$	mass of solid impregnated with solvent, kg
$m_{ss}$	mass of solid after elimination of solvent, kg
$n$	angular velocity, $\text{s}^{-1}$
$R_p$	particle size, m
$\bar{R}_p$	mean particle size defined in Eq. (27), m
$t$	time, s
$t_{dif}$	characteristic diffusion time ( $= R_p^2/D_0$ ), s
$t_p$	characteristic penetration time ( $= R_p^2/D_0$ ), s
$X_{ap}$	apparent concentration in solid, kg solute/kg solid $\text{m}^{-3}$
$X_{ap}^*$	reduced concentration in solid, kg solute per unit actual volume $\text{m}^3/\text{kg}$ solute per unit volume at initial state $\text{m}^{-3}$
$X_s$	mass fraction in solid, kg solute/kg solid
$\bar{X}_s$	volume average fraction in solid, kg solute/kg solid
$X^*$	reduced fraction in solid, kg actual solute in solid/kg solute at initial state
$Y$	solute fraction in liquid, kg solute in liquid/kg solid
$Y^*$	reduced solute fraction in liquid, kg solute in liquid/kg solute at initial state
$Y_{ap}$	apparent concentration in liquid, kg solute/kg actual liquid $\text{m}^3$
$Y_{ap}^*$	reduced concentration in liquid, kg solute per unit volume in liquid $\text{m}^3/\text{kg}$ solute per unit volume at initial state in solid $\text{m}^{-3}$
$Pe_D$	Peclet number, ( $= R_p U/D_0$ )
$V_1$	liquid phase volume, $\text{m}^3$
$V_s$	solid volume, $\text{m}^3$
$V_{s,av}$	average solid volume (for mean particle size), $\text{m}^3$



$V_{ls}$	solvent volume in solid hase pores, $\text{m}^3$
$V_{sl}$	apparent volume of solid, $\text{m}^3$
$V$	intraparticle solvent velocity, $\text{ms}^{-1}$
$U_r$	radial solvent velocity, $\text{ms}^{-1}$

### Greek Letters

$\beta$	phase ratio ( $= V_{ls}/V_1$ )
$\varepsilon_p$	internal porosity, $\text{m}^3\text{m}^{-3}$
$\rho_{ap}$	apparent density of particle, $\text{kg m}^{-3}$
$\rho_1$	solvent density, $\text{kg m}^{-3}$
$\xi$	liquid–solid ratio ( $= V_1/m_s$ ), $\text{m}^3\text{kg}^{-1}$
$\mu_n$	positive root of the characteristic equation in analytical solution
$\theta$	dimensionless time parameter, ( $= tU/R_p$ )
$\tau$	tortuosity factor, $\text{mm}^{-1}$
$v_V$	relative volume change, $\text{m}^3$ solvent in pores/ $\text{m}^3$ initial volume

### Superscripts

0	initial state
$\infty$	equilibrium state

### REFERENCES

1. Vrentas, J.S.; Vrentas, C.M. A general theory for diffusion in purely viscous binary fluid mixtures. *Chem. Eng. Sci.* **2001**, *56*, 4571–4586.
2. Triday, J.; Smith, J.M. Dynamic behavior of supercritical extraction of kerogen from shale. *AIChE J.* **1988**, *34* (4), 658–668.
3. Beloborodov, V.; Korganashvili, V.; Voronenko, B. Equation of isothermal extraction in solid–liquid system. *J. Appl. Chem.* **1979**, *52* (10), 2233–2237.
4. Brunowska, A.; Brunowski, P.; Ilavski, J. Estimation of the diffusion coefficient from sorption measurements. *Chem. Eng. Sci.* **1977**, *32* (3), 717–722.
5. Arvind, G.; Bhatia, S.K. Determination of concentration-dependent adsorbate diffusivities by numerical inversion. *Chem. Eng. Sci.* **1995**, *50* (8), 1361–1372.
6. Simeonov, E.; Tsibranska, I.; Minchev, A. Solid–liquid extraction from plants—experimental kinetics and modelling. *Chem. Eng. J.* **1999**, *73*, 255–259.
7. Axelrood, G.A.; Altsuler, M.A. Diffusion in capillary-porous media. In



*Introduction in Capillary Chemical Technology*, 1st Ed.; Chimia: Moscow, 1983; 116–120.

8. Crank, J. *The Mathematics of Diffusion*; Claderon Press: Oxford, 1975.
9. Seikova, I.; Guiraud, P.; Mintchev, A. Experimental study of the solid phase deformation during extraction of Belladone radix. *Dokl. Bolg. akad. nauk* **2000**, *53* (3), 55–58.
10. Grishina, M.S.; Kovalenko, L.I.; Popov, D.M. Atropine and scopolamine essays in belladone tincture. *Farmatsiya (Moscow)* **1986**, *35* (2), 24–27.
11. Sokolov, A.V.; Popov, D.M. Extraction spectrophotometry of alkaloids in raw belladone. *Farmatsiya (Moscow)* **1989**, *38* (6), 62–65.
12. Minchev, A.; Minkov, S. A model for determination of the effective diffusion by the standard function technique. *J. Appl. Chem.* **1984**, *57* (3), 717–720.
13. Stroescu, M.; Dobre, T.; Octavian, Fl. Differential solid–liquid extraction of sulfur from volcanic-type ore. *Chem. Eng. J.* **1999**, *54*, 717–723.

Received August 2002

Revised March 2003

